

Lightning transient analysis in wind turbine blades

A. Candela Garolera, J. Holboell, S. F. Madsen

Abstract—The transient behavior of lightning surges in the lightning protection system of wind turbine blades has been investigated in this paper. The study is based on simulation models consisting of electric equivalent circuits with lumped and distributed parameters involving different lightning current waveforms. The aim of the simulations is to study the voltages induced by the lightning current in the blade that may cause internal arcing. With this purpose, the phenomenon of current reflections in the lightning down conductor of the blade and the electromagnetic coupling between the down conductor and other internal conductive elements of the blade is studied. Finally, several methods to prevent internal arcing are discussed in order to improve the lightning protection of the blade.

Keywords: Lightning surge, wind turbine blades, lightning protection, overvoltage, current reflection, modeling.

I. INTRODUCTION

WIND turbines are especially vulnerable to lightning strikes due to their height and location in isolated areas. In particular the rotor blades are known to receive several lightning strikes through the wind turbine life time [1]. During the past couple of years many manufacturers, and especially wind turbine owners, have experienced a large increase in the cost related to lightning damages. Insurance companies insuring large wind farms, also find that a large share of their insurance claims is linked to lightning damages on the blades. Therefore an efficient lightning protection system is essential to prevent structural damages in the blade in the event of lightning strike.

The main components of the lightning protection system of a wind turbine blade are the air termination system and the transmission system. The air termination usually comprises one or more receptors along the blade and the transmission system consists of a down conductor connecting the receptors to the root of the blade. Even though an efficient air termination system is decisive in order to avoid direct strikes on the blade surface, the role of the transmission system is also critical. When lightning discharges strike the receptor, the current surge that travels along the down conductor may induce high voltages and currents in any other conductive component of the blade [1]. These conductive elements may be electrical wiring for measuring purposes, de-icing systems

or carbon fiber laminate if it is included in the blade structure. Considering that internal arcing between the down conductor and the other conductors can involve severe damages in the blade structure, the separation distances and equipotential bonding between conductors must be carefully studied.

In this paper, the voltage induced by lightning in the wind turbine blade is investigated by simulations based on electric equivalent circuits. When building the equivalent circuit of the lightning down conductor, the question of whether to model it with lumped circuit or as transmission line arises. In general, the necessity of a transmission line model is dependent on the steepness of the voltage/current signal applied and the length of the line. Field measurements have shown that when there is a lightning strike at the top of a tall tower, the current waveform may change due to the presence of current reflections [2]. The increasing height of the wind turbines suggests that current reflections may as well appear in the wind turbine blades [3].

Two models are developed in this paper, both described in section II. The first model is intended to determine the significance of the lightning current reflections in the blade down conductor, and evaluate the accuracy of lumped circuits versus the transmission line approach. The second model studies the case of an electric wire running in parallel with the blade down conductor, and it is therefore focused on the electromagnetic coupling between them. The equivalent circuit used in this model is based on the outcome of the first model.

The electric parameters used in the equivalent circuits are determined with the finite element method and can be found in section III. Time domain simulations based on the equivalent circuits are performed using the simulation software PSCAD and the results are summarized in section IV.

Finally, the outcome of the simulations is analyzed in section V, where different methods to reduce the probability of undesirable sparking inside the blade are discussed.

II. MODELS

The voltages induced by the lightning current within the blade are determined through two models, described in sections II.A and II.B, respectively. The wind turbine blade used in both models has a length of 60m, and it is equipped with a punctual receptor at the tip and a down conductor running from the tip to the root (Fig. 1).

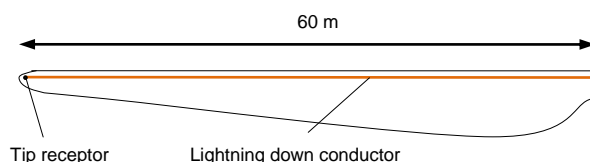


Fig.1. Blade used in the simulations: 60 m long, equipped with a lightning tip receptor and a down conductor.

Anna Candela Garolera and Joachim Holboell are with the Technical University of Denmark, Department of Electrical Engineering, 2800 Kgs. Lyngby, Denmark
Søren Find Madsen is with Global Lightning Protection Services A/S, 4320 Lejre, Denmark.

A. Model 1. Blade lightning down conductor: π -lumped circuit vs. transmission line approach.

Model 1 comprises the whole path of the lightning current through the wind turbine, consisting of the blade down conductor, the tower and the grounding system.

The blade down conductor has been modeled using two different approaches. The first approach consists of a simple π -lumped circuit (Fig. 2a), where R_{LC} is the conductor resistance, L_{LC} is the conductor self-inductance and C_g the capacitance between the conductor and ground. In this approach the reflection of travelling waves is disregarded. In the second approach, the blade down conductor is modeled as a surge impedance Z_{LC} (Fig. 2b), consisting of the whole length of the blade. Z_{LC} is calculated from the expression (1), where R_{LC} and L_{LC} are the parameters as in the lumped circuit. This approach is intended to determine the reflections of the lightning wave. In order to simplify the circuit, in both cases the blade is considered in horizontal position with respect to ground, and therefore L_{LC} and C_g are assumed to be constant.

The wind turbine tower and the grounding system are modeled as surge impedances, based on simple models developed for transmission lines. The surge impedance of the tower Z_{tower} is calculated as a vertical cylinder (2) [4] and the surge impedance of the grounding Z_{ground} is determined for vertical electrodes (3)-(7) [5].

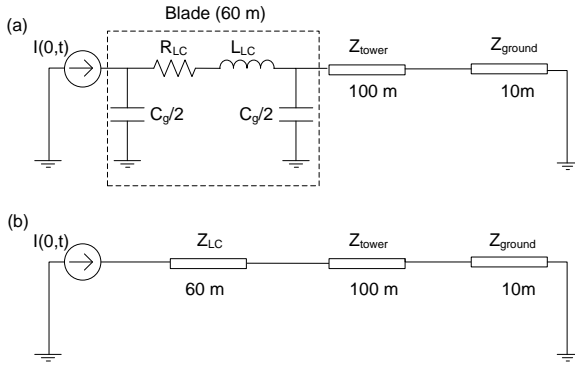


Fig.2.

Equivalent circuit of the wind turbine, where the blade is modeled (a) as a π -lumped circuit and (b) as a transmission line.

$$Z_{LC} = \sqrt{\frac{L_{LC}}{C_g}} \quad (1)$$

$$Z_{tower} = 60 \left(\ln \frac{2\sqrt{2}h}{r} - 2 \right) \quad (2)$$

$$Z_{ground} = Z_0 \coth \gamma \ell \quad (3)$$

$$Z_0 = \sqrt{\frac{j\omega L_g}{\frac{1}{R_g} + j\omega C_g}} \quad \gamma = \sqrt{j\omega L_g \left(\frac{1}{R_g} + j\omega C_g \right)} \quad (4)$$

$$R_g [\Omega \cdot m] = \frac{\rho}{2\pi} \left(\ln \frac{4\ell}{a} - 1 \right) \quad (5)$$

$$L_g [H / m] = \frac{\mu}{2\pi} \left(\ln \frac{2\ell}{a} - 1 \right) \quad (6)$$

$$C_g [F / m] = \frac{\rho \epsilon}{R \ell} \quad (7)$$

The terms used in expressions (2)-(7) as well as the values assigned for the simulations can be found in section III.

B. Model 2: Electromagnetic coupling: blade lightning conductor – internal electrical wire

Model 2 consist of the lightning down conductor and an internal electrical wire running in parallel along the blade. The wire is part of a measuring system and it is connected to an assumed electronic device placed at the root of the blade (Fig. 3).

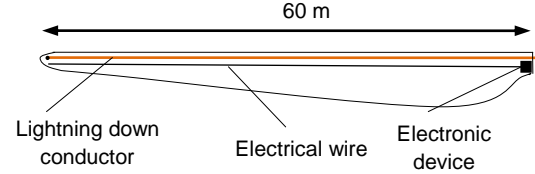


Fig.3. Geometry of Model 2: Blade equipped with lightning down conductor and internal electrical wire connected to an electronic device.

Two cases are studied. In case 1 the wire is connected to the lightning down conductor at the root of the blade, ensuring similar potential of the down conductor and the panel containing the electronic device. In case 2 the device is floating. In order to prevent side flashes between conductor and wire, the wire is installed as far as possible from the lightning conductor. Therefore, the distance between them assumed in the calculations is 0.2m at the tip and 1.5m at the root of the blade, and it changes linearly along the blade.

According to the simulation results of Model 1 (section IV), the π -lumped approach is considered appropriate for the equivalent circuit of Model 2 and the transients in question here. Since the current reflections are disregarded, there is no need for including the wind turbine tower and the grounding system in Model 2.

The equivalent circuit is modeled with 12 π -sections, each representing a length Δx of 5 m of the blade (Fig. 4). The aim of dividing the circuit in several sections is to be able to measure the current and voltage in different points along the blade length. The values of resistances R_{LC} and R_w , inductances L_{LC} and L_w and mutual inductive and capacitive coupling M and C can be found in section III.

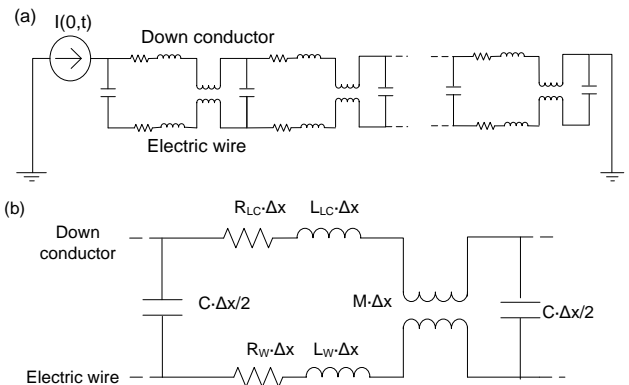


Fig.4. (a) Equivalent circuit of Model 2, (b) Single 5-meter section of Model 2, consisting of the resistance and inductance of the lightning conductor and internal electrical wire, and their inductive and capacitive coupling .

C. Lightning current waveforms

The current waveforms used for the simulation correspond to the maximum values of lightning parameters for the first positive, negative and subsequent strokes, according to [1]. In the simulations, the lightning surge is modeled using the Heidler function (8) instead of the double exponential commonly employed in lightning simulations. The purpose is to avoid the infinitely high rate of current change at $t=0$ found in the double exponential waveform, which may erroneously lead to too high induced voltages [6].

$$i(0,t) = \frac{I_0}{\eta} \cdot \frac{\left(\frac{t}{\tau_1}\right)^n}{1 + \left(\frac{t}{\tau_1}\right)^n} \cdot e^{-\left(\frac{t}{\tau_2}\right)} \quad (8)$$

I_0 , η , n , τ_1 and τ_2 are the parameters that define the current peak, the rise time and the decay time. The values assigned for the simulations can be found in section III.

III. PARAMETERS OF THE MODELS

The calculation of the electrical parameters depends on the geometry and material properties of the conductive components in the models. Table I and Table II show the geometry and material properties assigned to Model 1 and Model 2 respectively.

TABLE I
GEOMETRY OF THE CONDUCTIVE COMPONENTS IN MODEL 1

Blade conductor length	l_c	60 m
Blade conductor radius	r_c	4 mm
Tower height	h	100 m
Tower radius	r	3 m
Ground electrode length	ℓ	10 m
Ground electrode radius	a	30 mm
Copper resistivity	ρ_c	1.67e-8 $\Omega \cdot m$
Ground resistivity	ρ_g	100 $\Omega \cdot m$

TABLE II
GEOMETRY OF THE CONDUCTIVE COMPONENTS IN MODEL 2

Blade conductor length	l_c	60 m
Blade conductor radius	r_c	4 mm
Blade electrical wire length	l_w	60 m
Blade electrical wire radius	r_w	1 mm
Distance conductor-wire at the tip of the blade	d_{tip}	0.2 m
Distance conductor-wire at the root of the blade	d_{root}	1.5 m
Copper resistivity	ρ_c	1.67e-8 $\Omega \cdot m$

The electrical parameters of the tower and grounding are determined with expressions [2]-[7], using the values from Table I. The parameters of the blade conductors are determined by numerical calculation with the finite element method (FEM). The FEM models depend on the geometry, material characteristics of the conductors and the frequency in

the case of the electrical resistance. In order to take into account the skin effect in the conductors, the resistances R_{LC} and R_w have been calculated for the equivalent main frequency of the lightning impulses wave-front. The frequencies used are 25 kHz, 250 kHz and 1 MHz, corresponding to the first positive, negative and subsequent stroke respectively.

Table III and Table IV show the electrical parameters used in Model 1 and Model 2 respectively.

TABLE III
ELECTRICAL PARAMETERS OF MODEL 1

R_{LC} 25kHz	1.73 m Ω/m
R_{LC} 250kHz	5.44 m Ω/m
R_{LC} 1MHz	11.4 m Ω/m
L_{LC}	1.55 $\mu H/m$
C_g	7.21 pF/m
Z_{LC}	463.66 Ω
Z_{tower}	152.78 Ω
R_{tower}	0.028 m Ω/m
Z_{ground}	63.93 Ω
R_{ground}	0.98 Ω/m

TABLE IV
ELECTRICAL PARAMETERS OF MODEL 2

R_{LC} 25kHz	1.73 m Ω/m
R_{LC} 250kHz	5.44 m Ω/m
R_{LC} 1MHz	11.4 m Ω/m
L_{LC}	1.55 $\mu H/m$
C_g	7.21 pF/m
R_w 25kHz	7.95 m Ω/m
R_w 250kHz	22.2 m Ω/m
R_w 1MHz	43.0 m Ω/m
L_w	1.85 $\mu H/m$
M at d_{tip}	0.78 $\mu H/m$
M at d_{root}	0.38 $\mu H/m$
C at d_{tip}	3.94 pF/m
C at d_{root}	1.60 pF/m

Table V shows the parameters of the current waveforms used in the simulations, corresponding to the first positive, negative and subsequent stroke. These lightning waveforms are defined by the peak of current, the duration of the wave-front and the decay time until half the current peak.

TABLE V
CHARACTERISTICS OF LIGHTNING CURRENT WAVEFORMS

Lightning stroke	1 st positive	1 st negative	Subsequent
Current peak [kA]	200	100	50
Rise time [μs]	10	1	0.25
Decay time to half value [μs]	350	200	100

IV. RESULTS

This section summarizes the results of the simulations based on Model 1 and Model 2.

A. Model 1: Blade lightning down conductor: π -lumped circuit vs. transmission line approach.

The current impulses are injected at the tip receptor and the voltage drop is measured between the receptor and the down conductor at the root of the blade (Fig. 5). The voltage drop for both the π -lumped circuit and the surge impedance approximations has been represented together in Fig. 6-8.

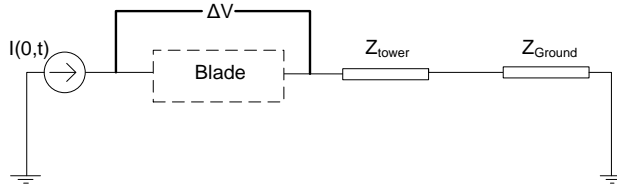


Fig.5. Model 1: Voltage drop across the lightning down conductor when the lightning current is injected.

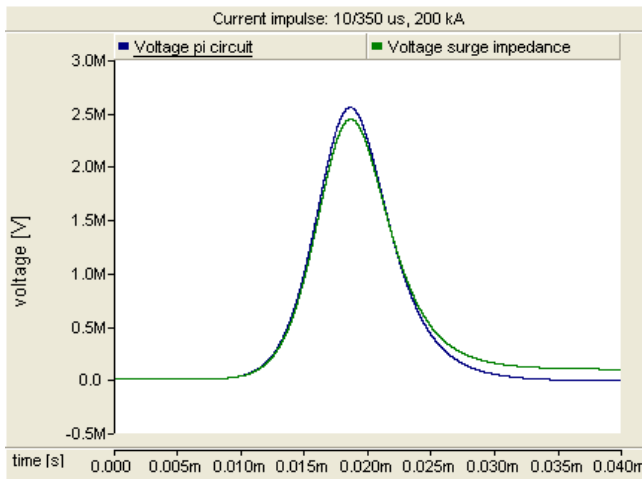


Fig.6. Model 1: Voltage drop across the lightning down conductor of the blade for the π -lumped circuit (blue trace) and the transmission line (green trace). Current impulse corresponding to the first return stroke positive.

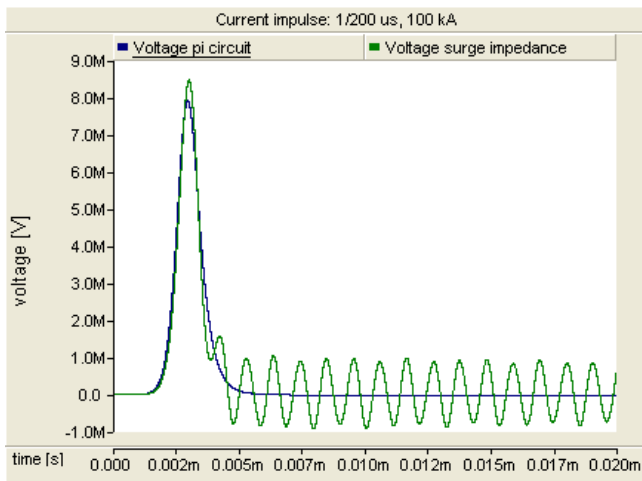


Fig.7. Model 1: Voltage drop across the lightning down conductor of the blade for the π -lumped circuit (blue trace) and the transmission line (green trace). Current impulse corresponding to the first return stroke negative.

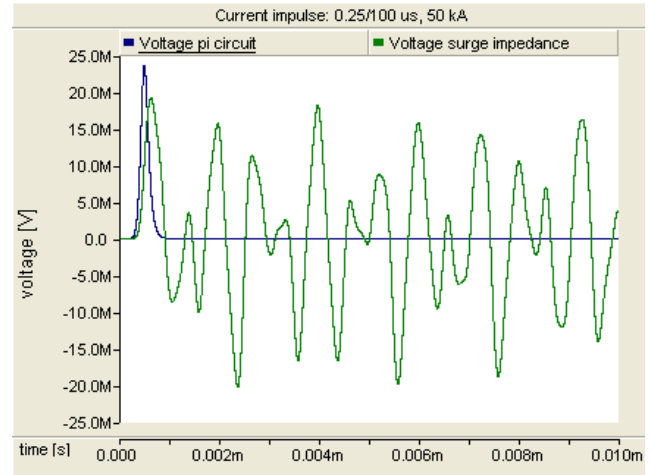


Fig.8. Model 1: Voltage drop across the lightning down conductor of the blade for the π -lumped circuit (blue trace) and the transmission line (green trace). Current impulse corresponding to the subsequent return stroke.

Figs. 6-8 show that the lightning conductor only needs to be modeled as a transmission line for current rise times up to $1\mu\text{s}$. When applying the first positive return stroke, with a rise time of $10\mu\text{s}$, there are no reflections and similar results are obtained from both models (Fig. 6). However, when applying the waveform of the first negative return stroke, with a rise time of $1\mu\text{s}$, the reflections are in the order of 10% of the main peak voltage (Fig. 7), and for the subsequent return stroke, with a rise time of $0.25\mu\text{s}$, the reflections are significantly higher, similar to the main peak voltage (Fig. 8). According to the field observations, only 5% of the lightning first return and subsequent stroke have a rise time lower than $1.8\mu\text{s}$ and $0.22\mu\text{s}$ respectively [7]. It is also observed that, even in the case of the subsequent stroke, the voltage of the reflections do not exceed the first voltage peak (Fig. 8). Therefore, the π lumped circuit is considered acceptable to calculate the maximum peaks of voltage in Model 2 (section IV.B). The advantage of using the π lumped circuit to represent the lightning down conductor is that it can be divided in several sections and different electric parameters can be assigned to each section. This is especially interesting when the geometry of the model varies with the length. For this reason, the π lumped circuit has been used in Model 2.

B. Model 2: Electromagnetic coupling: blade lightning conductor – internal electrical wire

The current impulses are injected in the receptor at the tip of the blade. The current induced in the internal wire and the voltage difference between the down conductor and the wire is measured for Case 1, where the wire is connected to the down conductor at the root of the blade, and for Case 2, where the wire is floating. The current and voltage are measured in each π -section of the circuit (Fig. 9).

Fig. 10-12 show the peak of current induced in the internal wire along the blade length for Case 1 and Case 2, where 60 m corresponds to the tip of the blade and 0 to the root.

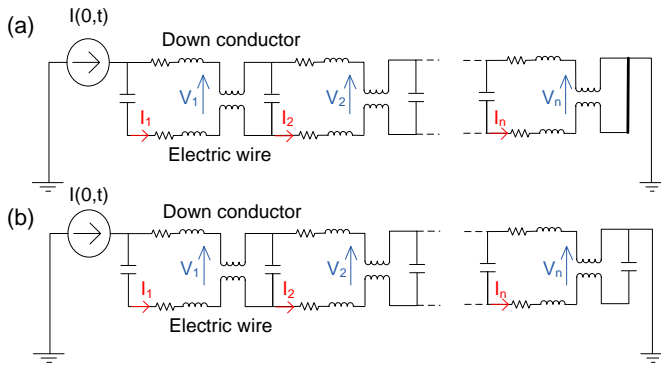


Fig.9. Model 2: Voltage and current measurements in (a) case 1, equipotential bonding between the wire and the down conductor at the root of the blade and (b) floating wire

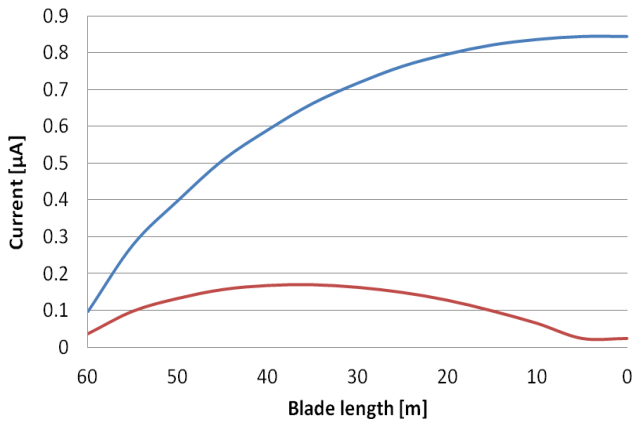


Fig.10. Maximum value of current induced in the wire for case 1: wire connected at the root (blue trace) and Case 2: wire floating (red trace). Current impulse corresponding to the first return stroke positive.

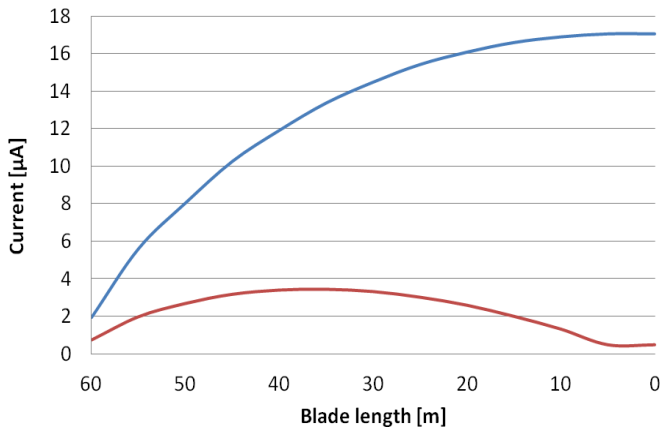


Fig.11. Maximum value of current induced in the wire for case 1: wire connected at the root (blue trace) and Case 2: wire floating (red trace). Current impulse corresponding to the first return stroke negative.

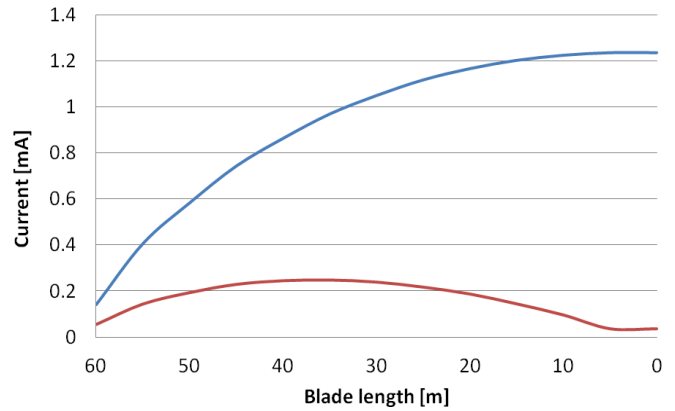


Fig.12. Maximum value of current induced in the wire for case 1: wire connected at the root (blue trace) and Case 2: wire floating (red trace). Current impulse corresponding to the subsequent return stroke.

It is observed in Figs. 10-12 that the induced current in case 2, where the wire is floating, is considerably lower than in case 1. In both cases, the induced current in the wire is higher as shorter the rise-time of the lightning impulse, reaching a maximum close to 1.2 mA in case 1 and 0.25 mA in case 2 for the subsequent return stroke.

Figs. 13-15 show the voltage difference V [MV] between the lightning conductor and the wire along the blade in case 1, where the wire is connected to the down conductor at the root of the blade. The blade length 60 corresponds to the tip of the blade and 0 to the root. The average electric field between the conductor and the wire, calculated as the voltage difference divided by the distance between them, is also included in the graphs.

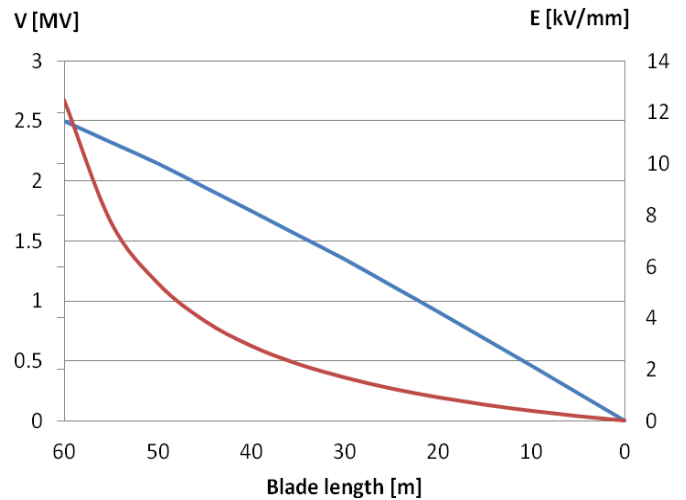


Fig.13. Maximum voltage difference V [MV] between the lightning conductor and the wire (blue trace) and average electric field E [kV/mm] (red trace) for case 1. Current impulse corresponding to the first return stroke positive.

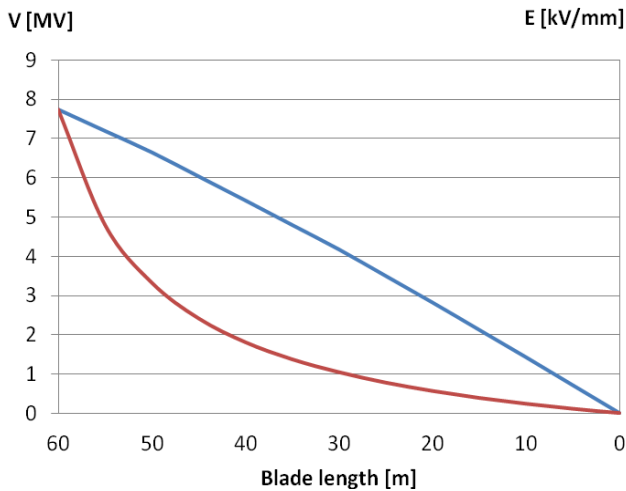


Fig. 14. Maximum voltage difference V[MV] between the lightning conductor and the wire (blue trace) and average electric field E [kV/mm] (red trace) for case 1. Current impulse corresponding to the first return stroke negative.

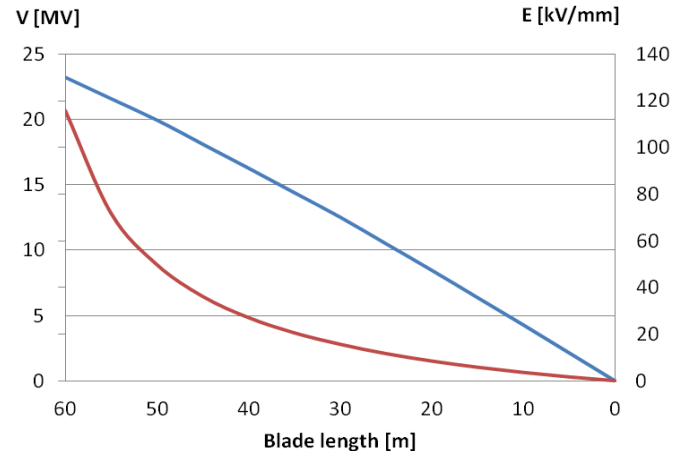


Fig. 15. Maximum voltage difference V[MV] between the lightning conductor and the wire (blue trace) and average electric field E [kV/mm] (red trace) for case 1. Current impulse corresponding to the subsequent return stroke.

Figs. 13-15 show that the maximum value of the voltage is reached at the tip of the blade, and decreases when approaching the root. As expected, the voltage also depends on the waveform, and is becoming higher as shorter the rise time of the applied current waveform is. It is especially interesting to look at the average electric field between both conductors, since it determines the risk of side flashes. For case 1, the electric field at the tip of the blade is around 12 kV/mm for the first positive stroke, 40 kV/mm for the first positive stroke, and 120 kV/mm for the subsequent stroke. Considering 0.5kV/mm as the breakdown strength of the air in a wet and polluted blade cavity, in all three cases there is risk of internal arcing between the lightning conductor and the wire.

Figs. 16-18 show the voltage difference V [MV] between the lightning conductor and the wire along the blade in case 2, where the wire is floating

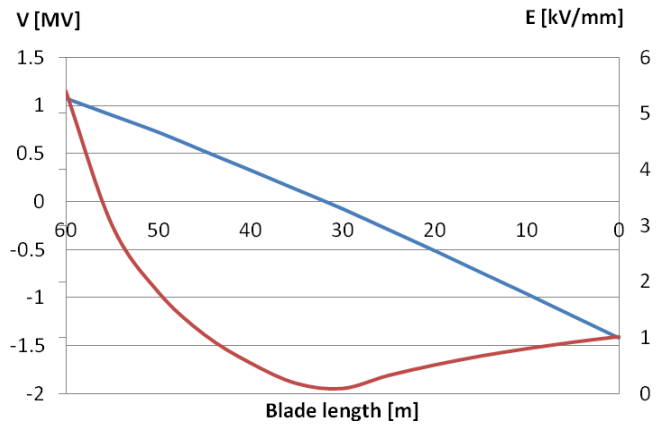


Fig. 16. Maximum voltage difference V[MV] between the lightning conductor and the wire (blue trace) and average electric field E [kV/mm] (red trace) for case 2. Current impulse corresponding to the first return stroke positive.

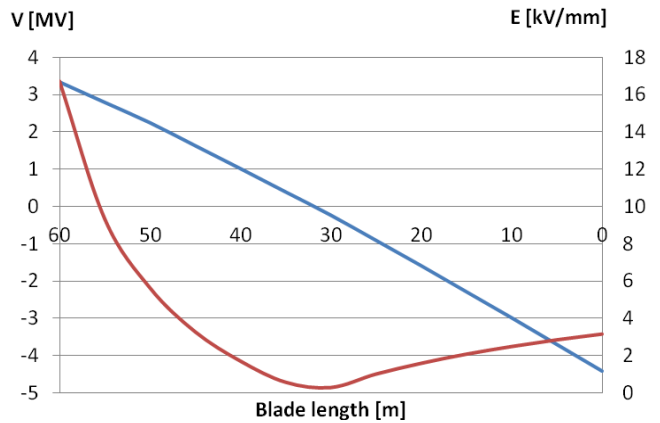


Fig. 17. Maximum voltage difference V[MV] between the lightning conductor and the wire (blue trace) and average electric field E [kV/mm] (red trace) for case 2. Current impulse corresponding to the first return stroke negative.

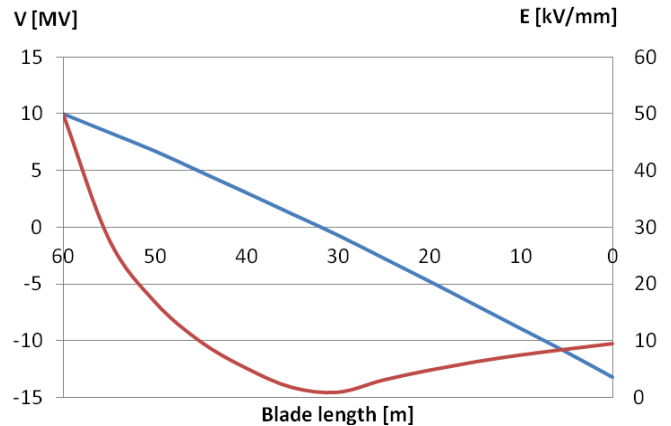


Fig. 18. Maximum voltage difference V[MV] between the lightning conductor and the wire (blue trace) and average electric field E [kV/mm] (red trace) for case 2. Current impulse corresponding to the subsequent return stroke.

It is observed in Figs. 16-18 that the voltage difference between conductors in case 2 is lower than in case 1 and that it changes polarity in the middle of the blade. Due to this change of polarity, the electric field between conductors is lower than in case 1. However, the electric field at the tip of the blade is

around 5 kV/mm, 16 kV/mm and 50 kV/mm for the positive, negative and subsequent stroke respectively. Therefore, in all three cases there is still risk of internal arcing between the lightning conductor and the wire.

V. DISCUSSION

The simulations of Model 1 reveal that voltage reflections are only significant when the applied current waveform has a rise time less than 1 μ s. The probability of a natural lightning with such a fast rise time is low and the maximum voltage level of the reflections in the worse case does not exceed the first voltage peak. Therefore, the π -lumped approximation is considered acceptable for the simulation of the blade conductors, in order to determine the maximum peaks of voltage.

In Model 2, the electric field between conductors generated by the current impulses exceeds the breakdown strength of the air in all cases. Therefore insulation should be provided all along the conductors. Considering that the fiberglass has a dielectric strength around 20kV/mm [8], installing the cable in opposite sides of the blade structural webs would be a possible solution to avoid flashover.

It is also observed in Model 2 that the rise time of the applied current waveform has a strong influence both on the induced current and the voltage difference between conductors due to their inductive coupling. In this sense, the subsequent return stroke could be regarded as the most dangerous regarding internal arcing, even with a current peak lower than the first return stroke. However, the voltages in the wire induced by the subsequent return stroke have an approximate duration of 0.1 μ s. The electric breakdown depends both on the voltage level and the duration of the impulse, therefore it has to be studied if this extremely fast voltage peak may generate flashover between the two conductors.

Comparing the results of case 1 and 2, it is observed that both the induced current and the voltage differences are significantly lower when the electronic device is floating. However, in case of high current flowing along the wire due to direct lightning strike or side flashes from the lightning cable, the current may be transmitted to the electronic device causing severe damage. This situation is prevented in case 1, where the current would be derived to the lightning protection system before reaching the electronic device. An intermediate solution to keep the wire floating but being able to derive the high current from the wire to the down conductor could be to replace the equipotential connection with a surge arrester.

VI. CONCLUSIONS

Wind turbine blades include sensors and other electronic devices, such as de-icing or beacon systems, which usually require electrical wiring running in parallel with the lightning down conductor along the blade. In the event of lightning strike, the voltage differences between conductors may lead to internal arcing. The present investigations show simulations of the induced voltages and currents in the blade using electric

equivalent circuits as a useful tool to identify the critical voltage differences between conductive elements within the blade. Possible countermeasures to reduce the probability of undesirable sparking inside the blade are the increase of the separation distances between conductors, the insulation of conductors, the equipotential bonding and the use of surge arresters. The application of these measures will prevent damages on the electronic devices and other equipment, and it will therefore improve the lightning protection of the blade structure.

VII. REFERENCES

- [1] "IEC 61400-24 Ed.1.0: Wind turbines – Part 24: Lightning protection", IEC, June 2010
- [2] V. A. Rakov, "Transient response of a tall object to lightning," IEEE Transactions on Electromagnetic Compatibility, vol. 43, no. 4, Nov. 2001.
- [3] F. Rachidi *et al.* "A Review of Current Issues in Lightning Protection of New-Generation Wind-Turbine Blades", IEEE Transactions on Industrial Electronics, Vol. 55, No. 6, June 2008
- [4] T. Hara, O. Yamamoto "Modelling of a transmission tower for lightning surge analysis," IEE Proceedings on Generation, Transmission and Distribution, Vol. 143, Issue 3.
- [5] L. Grcev, "Modeling of Grounding Electrodes under Lightning Currents," IEEE Transactions on Electromagnetic Compatibility, vol. 51, no. 3, Aug. 2009.
- [6] F. Heidler, J. M. Cvetic, B. V. Stanic, "Calculation of Lightning Current Parameters" IEEE Transactions of Power Delivery, vol. 14, no. 2, Abr. 1999.
- [7] Uman, M.A. "The lightning discharge", Dover publications Inc., 2001
- [8] Madsen, S.F. "Interaction between electrical discharges and materials for wind turbine blades – particularly related to lightning protection" Ørsted – DTU, Electric Power Engineering, Technical University of Denmark, PhD thesis 2006